YMTHE, Volume *29*

Supplemental Information

Microglial vesicles improve post-stroke recovery by preventing immune cell senescence and favoring oligodendrogenesis

Stefano Raffaele, Paolo Gelosa, Elisabetta Bonfanti, Marta Lombardi, Laura Castiglioni, Mauro Cimino, Luigi Sironi, Maria P. Abbracchio, Claudia Verderio, and Marta Fumagalli

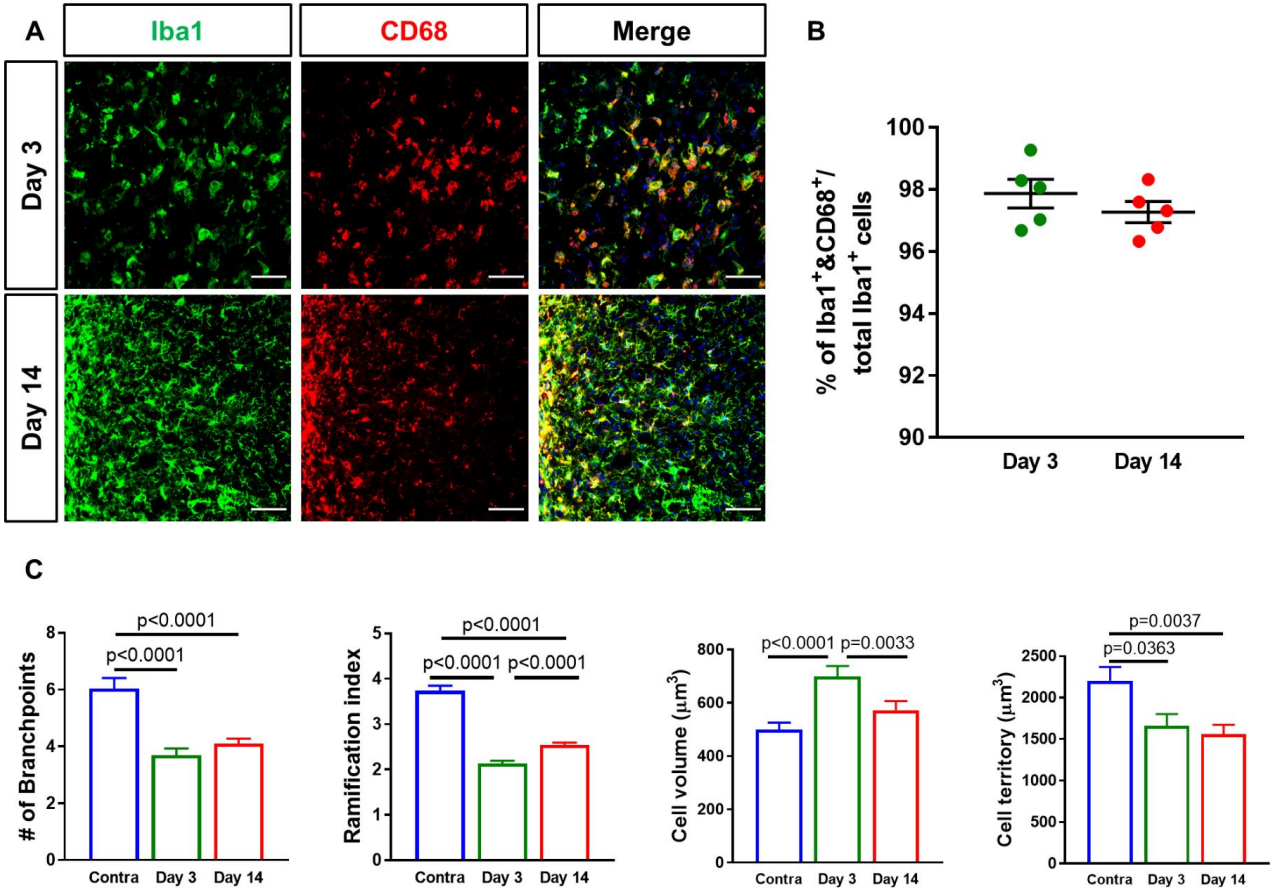

Figure S1. Iba1⁺ cells in the peri-infarct area express the scavenger receptor CD68 and undergo progressive morphological changes. (A) Representative images of Iba1⁺&CD68⁺ cells at the boundary of ischemic lesion (0-500 µm) at day 3 and 14 after MCAo. Scale bar: 50 µm. **(B)** Quantification of the percentage of Iba1⁺ cells co-expressing the scavenger receptor CD68 at the boundary of ischemic lesion (0-500 µm) at day 3 and 14 post-MCAo (n=5). Data are expressed as mean ± SE. **(C)** Quantification of Iba1⁺ cells number of branchpoints, ramification index, cell volume and cell territory at the boundary of ischemic lesion (0-500 µm) at day 3 and day 14 post-MCAo and in the corresponding region of the contralateral hemisphere at day 1 post-MCAo (130-150 cells from 3 animals/experimental condition have been analyzed). Data are expressed as mean ± SE. Kruskal-Wallis test followed by Dunn's post-hoc analysis.

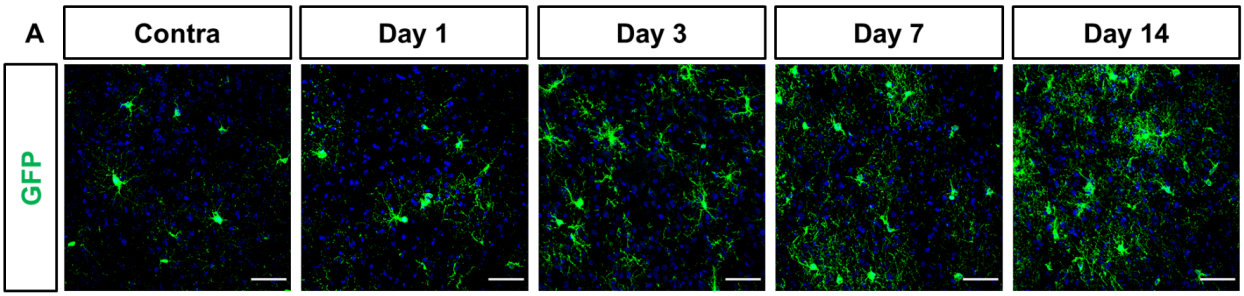

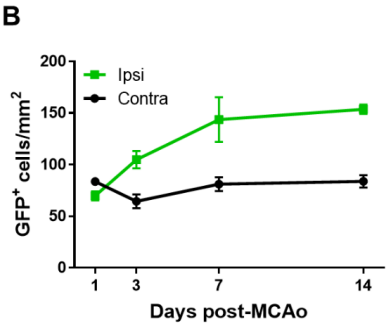

Ipsi vs Contra	p value
Day 1	ns
Day 3	0.0316
Day 7	0.0010
Day 14	0.0003

Days (ipsi)	p value
1 vs 3	ns
1 vs 7	0.0002
1 vs 14	<0.0001
3 vs 7	0.0459
3 vs 14	0.0103
7 vs 14	ns

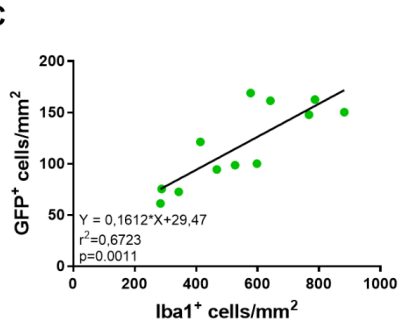

Figure S2. GFP⁺ OPC density at injury borders increases over time after cerebral ischemia in parallel with microglia/macrophage activation. (A) Representative images of GFP⁺ OPCs at the boundary of ischemic lesion (0-500 µm) at day 1, 3, 7 and 14 after MCAo and in the corresponding region of the contralateral hemisphere at day 1 post-MCAo. Scale bar: 50 µm. **(B)** Quantification of the density of GFP⁺ OPCs at the boundary of ischemic lesion (0-500 µm) and in the corresponding region of the contralateral hemisphere at day 1, 3, 7 and 14 after MCAo (n=3). Data are expressed as mean ± SE. Two-way ANOVA (Interaction p=0.0017, Time p=0.0008, MCAo p<0.0001) followed by Tukey's post-hoc analysis (p values relative to multiple comparisons are reported in the tables). **(C)** Scatter plot representation of the linear correlation between the densities of Iba1⁺ cells (*x* axis) and GFP⁺ OPCs (*y* axis) at the boundary of ischemic lesion (0-500 µm) at the different time points analyzed after MCAo. For correlation analysis, two-tailed Pearson test was used.

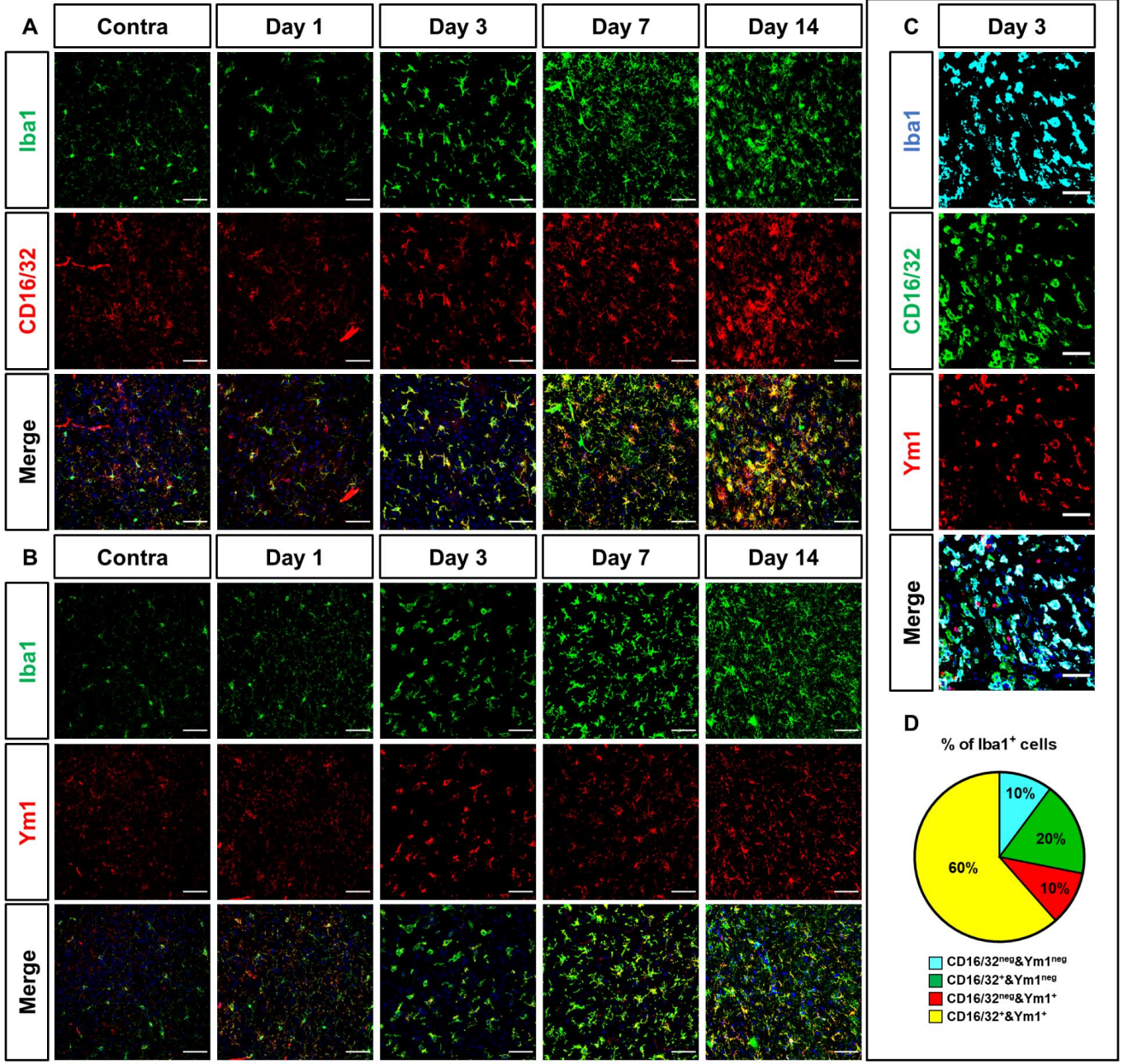

Figure S3. Characterization of Iba1⁺ co-localization with the pro-inflammatory marker CD16/32 or the pro-resolving factor Ym1 in the peri-infarct area. (A) Representative images of Iba1⁺&CD16/32⁺ cells at the boundary of ischemic lesion (0-500 µm) at day 1, 3, 7 and 14 after MCAo and in the corresponding region of the contralateral hemisphere at day 1 post-MCAo. Scale bar: 50 µm. **(B)** Representative images of Iba1⁺&Ym1⁺ cells at the boundary of ischemic lesion (0-500 µm) at day 1, 3, 7 and 14 after MCAo and in the corresponding region of the contralateral hemisphere at day 1 post-MCAo. Scale bar: 50 µm. **(C)** Representative images of triple positive Iba1⁺&CD16/32⁺&Ym1⁺ cells at the boundary of ischemic lesion (0-500 µm) at day 3 after MCAo. Scale bar: 50 µm. **(D)** Quantification of the percentage of Iba1⁺ cells co-expressing CD16/32, Ym1 or both markers at the boundary of ischemic lesion (0-500 µm) at day 3 after MCAo.

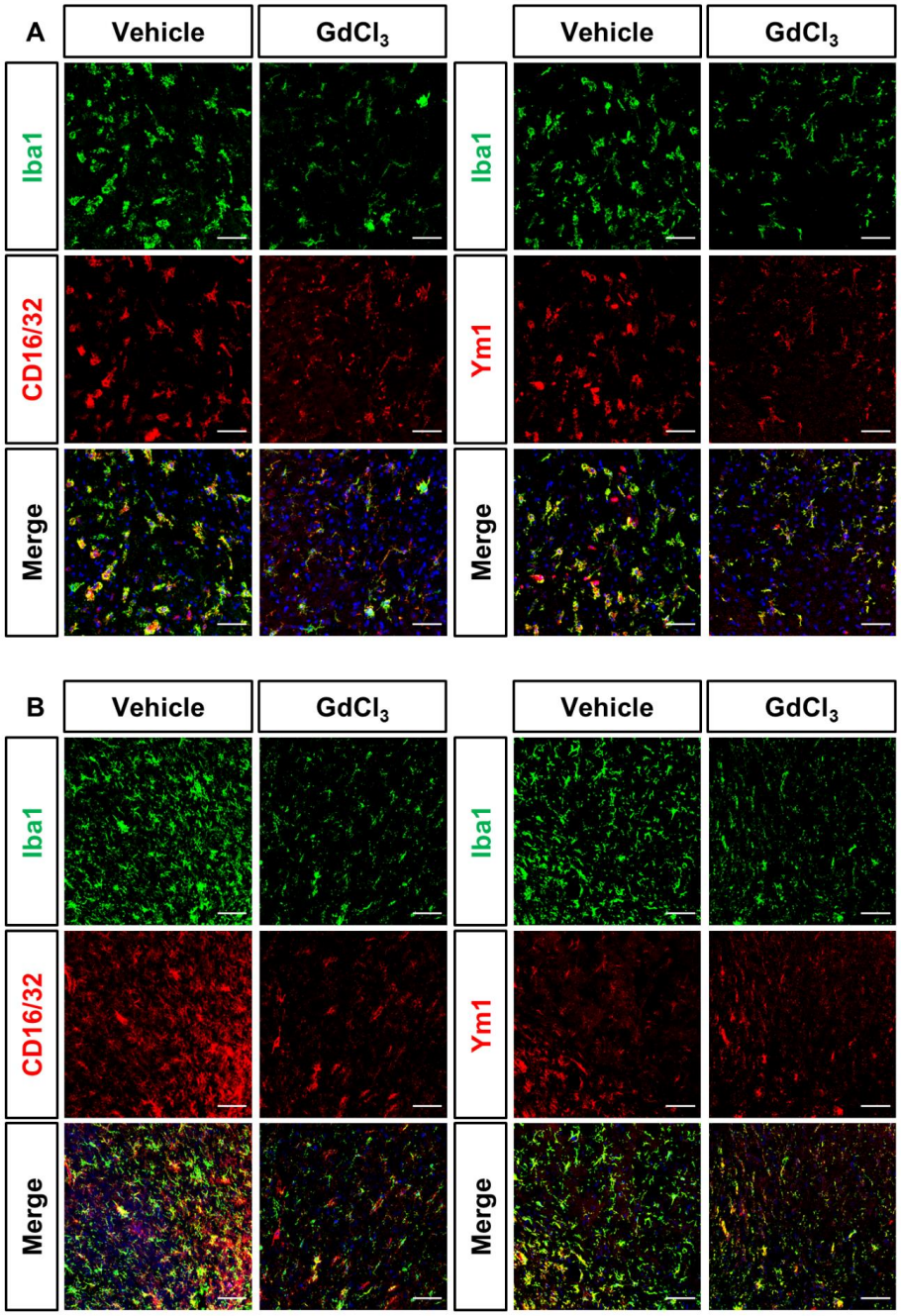

Figure S4. Characterization of Iba1 co-localization with CD16/32 or Ym1 after microglia/macrophage depletion during the early or late phase after MCAo. (A) Representative images of Iba1$^+$&CD16/32$^+$ and Iba1$^+$&Ym1$^+$ cells at the boundary of ischemic lesion (0-500 μm) at day 3 post-MCAo following intranasal administration of GdCl3 or vehicle. Scale bar: 50 μm. **(B)** Representative images of Iba1$^+$&CD16/32$^+$ and Iba1$^+$&Ym1$^+$ cells at the boundary of ischemic lesion (0-500 μm) at day 17 post-MCAo following intranasal administration of GdCl3 or vehicle. Scale bar: 50 μm.

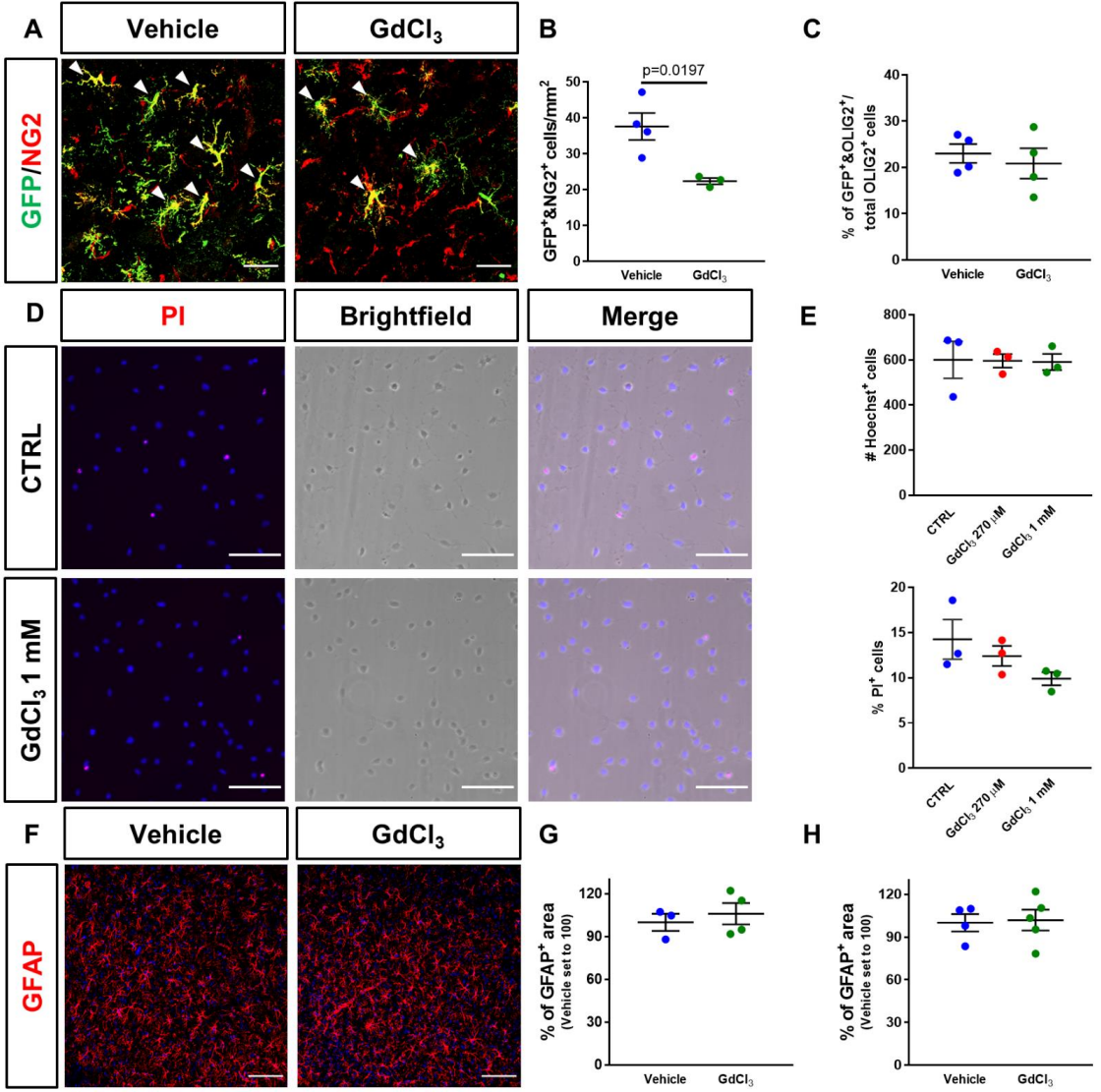

Figure S5. Microglia reduction by $GdCl_3$ treatment limits the recruitment of early GFP⁺ OPCs expressing NG2 at the boundary of ischemic lesion without exerting toxic effects on primary OPC cultures and on astrogliosis. (A) Representative images of GFP/NG2 staining at the boundary of ischemic lesion (0-500 µm) at day 3 post-MCAo following intranasal administration of $GdCl_3$ or vehicle. Arrowheads indicate cells co-expressing GFP and NG2. Scale bar: 50 µm. **(B)** Quantification of the density of GFP⁺&NG2⁺ cells at the boundary of ischemic lesion at day 3 post-MCAo following intranasal administration of $GdCl_3$ or vehicle. Data are shown as mean ± SE (n=4-3). Student's t-test. **(C)** Quantification of the percentage of Olig2⁺ cells labelled by GFP expression at the boundary of ischemic lesion at day 3 post-MCAo following early intranasal administration of $GdCl_3$ or vehicle (n=4). Data are expressed as mean ±SE. **(D)** Representative images of primary OPCs incorporating propidium iodide (PI) after treatment with $GdCl_3$ (1 mM) or medium alone (CTRL). Hoechst33258 was used to label cell nuclei. Scale bar: 50 µm. **(E)** Quantification of the number of Hoechst33258⁺ cell nuclei and of the percentage of PI⁺ apoptotic cell nuclei in primary OPC cultures exposed to $GdCl_3$ (270 µM or 1 mM) or CTRL. Data are shown as mean ± SE (n=3). **(F)** Representative images of GFAP staining at the boundary of ischemic lesion (0-500 µm) at day 3 post-MCAo following intranasal administration of $GdCl_3$ or vehicle. Scale bar: 100 µm. **(G)** Quantification of the percentage of GFAP⁺ area at the boundary of ischemic lesion at day 3 post-MCAo following early intranasal administration of $GdCl_3$ or vehicle (n=3-4). Data are expressed as mean ±SE. **(H)** Quantification of the percentage of GFAP⁺ area at the boundary of ischemic lesion at day 17 post-MCAo following late intranasal administration of $GdCl_3$ or vehicle (n=4-5). Data are expressed as mean ± SE.

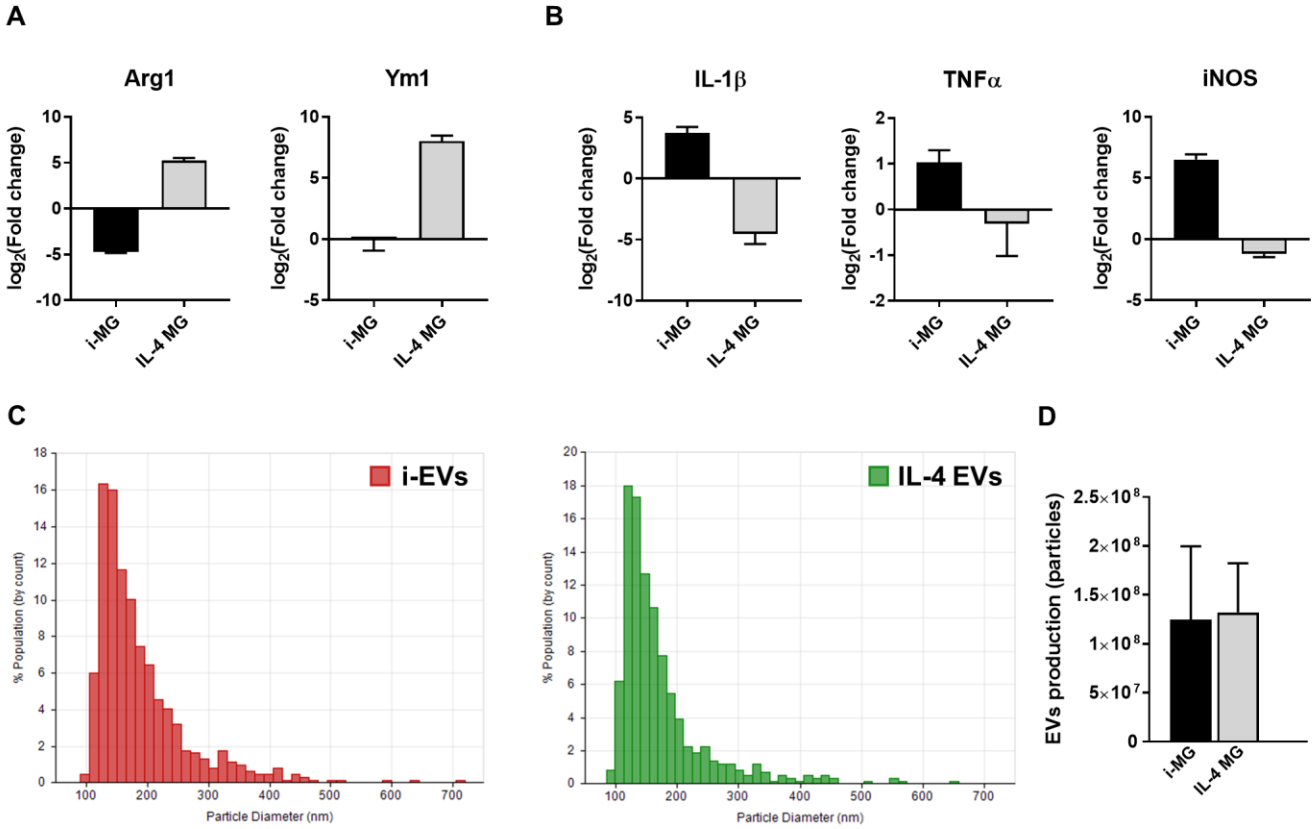

Figure S6. Characterization of polarization and EV release of murine microglia exposed to pro-inflammatory (i-MG) or pro-regenerative (IL-4 MG) stimuli. (A) Gene expression of pro-regenerative markers in primary microglia exposed to pro-inflammatory (i-MG) or pro-regenerative (IL-4 MG) stimuli with respect to non-stimulated cells (NS-MG) set to 0. Data are shown as mean ± SE. **(B)** Gene expression of pro-inflammatory markers in primary microglia exposed to pro-inflammatory (i-MG) or pro-regenerative (IL-4 MG) stimuli with respect to non-stimulated cells (NS-MG) set to 0. Data are shown as mean ± SE. **(C)** Size distribution graphs relative to EVs released by i-MG (i-EVs) and IL-4 MG (IL-4 EVs) upon ATP simulation. EV size was measured by Tunable Resistive Pulse Sensing (TRPS) technique. **(D)** Quantification of EVs produced by i-MG (i-EVs) and IL-4 MG (IL-4 EVs) upon ATP simulation. Data are expressed as mean ± SE.